Model and discretization impact on oscillatory optimal control for a diesel-electric powertrain

Martin Sivertsson * **Lars Eriksson** *

* *Vehicular Systems, Dept. of Electrical Engineering, Linköping University, SE-581 83 Linköping, Sweden, {marsi, larer}@isy.liu.se.*

Abstract: A mean value engine model is used to study optimal control of a diesel-electric powertrain. The resulting optimal controls are shown to be highly oscillating for certain operating points, raising the question whether this is an artifact of discretization, modeling choices or a phenomenon available in real engines. Several model extensions are investigated and their corresponding optimal control trajectories are studied. It is shown that the oscillating controls cannot be explained by the implemented extensions to the previously published model, nor by the discretization, showing that for certain operating points the optimal solution is periodic.

1. INTRODUCTION

The engine speed of a conventional vehicle is normally decided by the wheel speed and the gear ratio. In a diesel-electric powertrain this mechanical path between the combustion engine and the wheels is replaced by an electric path instead. This introduces an extra degree of freedom since the engine speed can be controlled independently of the wheel speed, which offers the potential of both optimizing the performance and consumption since the operating point of the diesel engine can be controlled more freely than in a conventional powertrain. This of course raises the question of how to use this extra degree of freedom.

Previously it has been studied how to optimally control the powertrain between two different power levels, see Sivertsson and Eriksson [2015a,b]. For off-highway machinery the driving patterns are normally very transient, something that is captured in the World Harmonized Transient Cycle (WHTC), see WHDC Working Group [2005], shown in Fig. 1. The WHTC can be divided into 11 traction phases, defined as the period between two idle periods, where idle is assumed to occur when the engine speed is the idle speed and no power is required. Here the phases where the engine is motored, i.e. $P_{gen} < 0$ are ignored and P_{gen} is in those cases set to zero.

To investigate the potential of the diesel-electric powertrain and how to best exploit the extra degree of freedom introduced by the electrification of the powertrain, minimizing fuel for the WHTC is cast as an optimal control problem (OCP). In a conventional powertrain WHTC prescribes both engine speed and output power, but here engine speed is a degree of freedom and also optimized. If this OCP is solved for phase 8 in the WHTC the resulting controls are very oscillatory, see Fig. 2, $t \in [670, 678], [684, 687]$. It is mentioned in Sivertsson and Eriksson [2015a] that the optimal solutions in transient optimal control of a diesel-electric powertrain are often oscillatory and in Asprion et al. [2014] the unconfirmed

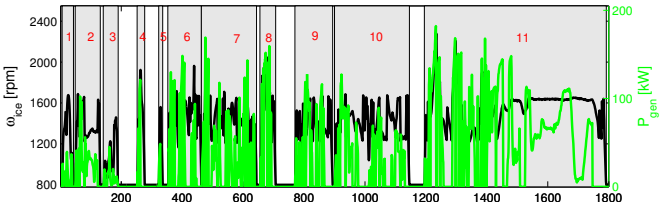

Fig. 1. The WHTC and its traction phases.

hypothesis is that the oscillations seen in the optimal variable geometry turbine (VGT) control of a diesel engine are due to decrease in the gas exchange losses. This is due to that the exhaust manifold pressure oscillates with the VGT position whereas the intake manifold pressure remains unaffected due to the slower turbocharger dynamics. This could indicate that the optimal solution is in fact periodical as described in Gilbert [1976], Gilbert [1977]. Other possible explanations are either that the solution is along a singular arc and that the controls are therefore oscillatory, as discussed in Schwartz [1996], or that it is an integration error exploited by the algorithm to decrease the criteria as shown in Hellström et al. [2010]. In both these cases it would be suspected that the frequency of the oscillations depend on the discretization. To test this hypothesis a single operating point is selected and studied using a very fine time discretization.

2. CONTRIBUTIONS

The contributions of this paper is a deeper study of the occurence of oscillating controls for diesel-electric powertrains as a solution for optimal control problems. More specifically it studies whether the observed oscillations are an artifact of the discretization. It also investigates if the oscillations can be explained by the models used and whether or not extending the model impacts the oscillating solutions. The paper also presents a fast and accurate residual gas model suitable for use in an optimal control context.

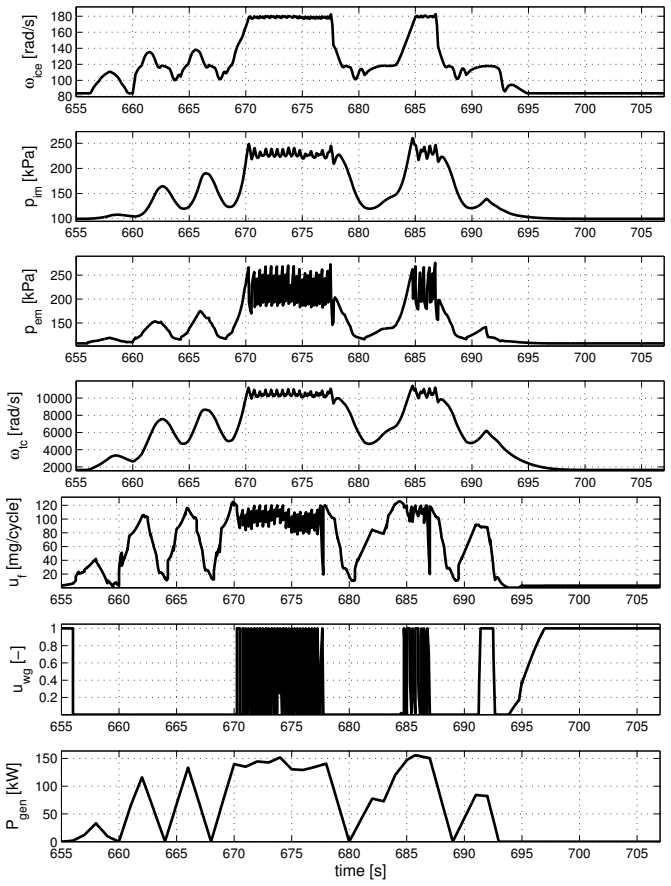

Fig. 2. The optimal solution to phase 8 of the WHTC, with ω_{ice} as a degree of freedom. The resulting controls are highly oscillatory, see $t \in [670, 678], [684, 687]$

Table 1. Symbols used

Symbol	Description	Unit
p	Pressure	Pa
T	Temperature	K
ω	Rotational speed	rad/s
$\dot{m}$	Massflow	kg/s
P	Power	W
M	Torque	Nm
E	Energy	J
Π	Pressure ratio	-
V	Volume	m^3
γ	Specific heat capacity ratio	-
c_p	Specific heat capacity constant pressure	J/(kg · K)
c_v	Specific heat capacity constant volume	J/(kg · K)
R	Gas Constant	J/(kg · K)
u_f, u_{wg}, P_{gen}	Control signals	mg/cycle, -, W
J	Inertia	kg · m^2
BSR	Blade speed ratio	-
ϕ	Fuel-air equivalence ratio	-
λ_{min}	Air-fuel smoke-limit	-
x_r	Residual gas fraction	-
MFR	Fuel to mass ratio	-
q_{HV}	Lower heating value	J/kg
r_c	Compression ratio	-

3. MODEL

The basic model used can be downloaded in the **LiU-D-El**-package from systems software [2014] and is described in detail as $MVEM_o$ in Sivertsson and Eriksson [2014]. The modeled diesel-electric powertrain consists of a 6-cylinder diesel engine with a fixed-geometry turbine and a wastegate for boost control, with a generator mounted on the output shaft. The states of the MVEM are engine and turbocharger speeds, $\omega_{ice/tc}$, and inlet and exhaust manifold pressures, $p_{im/im}$. The controls are injected fuel mass, u_f, wastegate position, u_{wg}, and generator power, P_{gen}. The engine model consists of two control volumes, intake and exhaust manifold, and four restrictions, compressor, engine, turbine, and wastegate. The governing differential equations of the MVEM are:

$$\frac{d\omega_{ice}}{dt} = \frac{P_{ice} - P_{mech}}{\omega_{ice} J_{GenSet}} \tag{1}$$

$$\frac{dp_{im}}{dt} = \frac{R_a T_{im}}{V_{im}} \left(\dot{m}_c - \dot{m}_{ac}\right) \tag{2}$$

$$\frac{dp_{em}}{dt} = \frac{R_e T_{em}}{V_{em}} \left(\dot{m}_{ac} + \dot{m}_f - \dot{m}_t - \dot{m}_{wg}\right) \tag{3}$$

$$\frac{d\omega_{tc}}{dt} = \frac{P_t \eta_{tm} - P_c}{\omega_{tc} J_{tc}} \tag{4}$$

For a complete list of the symbols used in the paper, see Table 1-2.

Table 2. Subscripts used

Index	Description	Index	Description
ice	Engine	$GenSet$	Engine-Generator
im	Intake manifold	em	Exhaust manifold
c	Compressor	ac	After compressor
t	Turbine	wg	Wastegate
f	Fuel	tc	Turbocharger
a	Air	e	Exhaust
gen	Generator-electrical	$mech$	Generator-mechanical
ref	Reference	$c, surge$	Compressor surge-limit
vol	Volumetric	d	Displaced
$fric$	Friction	$pump$	Pumping
ig	Indicated gross	eo	Engine out
amb	Ambient		

4. PROBLEM FORMULATION

This paper uses the MVEM to study optimal stationary operation, or lack of it in the case of oscillating controls.

4.1 Stationary optimization

As a reference for the dynamic optimization, three stationary optimization problems are first solved, to find the following three stationary points for the given ω_{ref}, P_{ref}-combination: The maximum efficiency, ϕ_{max}, the maximum fuel/air-ratio, η_{max}, and the minimum fuel/air-ratio, ϕ_{min}. $\eta = \frac{P_{gen}}{\dot{m}_f q_{HV}}$ is the efficiency of the powertrain and ϕ is the fuel/air-ratio. These problems are solved to find the optimal operating point for stationary operation and also the limits for stationary operation.

4.2 Dynamic optimization

The main optimal control problem studied is:

$$\begin{aligned} \min_{u(t)} \quad & \int_0^T \dot{m}_f \\ \text{s.t.} \quad & \dot{x}(t) = f(x(t), u(t)) \\ & (x(t), u(t)) \in \Omega(t) \end{aligned} \tag{5}$$

where x is the state vector of the MVEM, $\dot{x}$ is the state equations (1)-(4), and $u = [u_f, u_{wg}, P_{gen}]$. The optimal control problems are also subject to a set of constraints, namely:

$$
\begin{aligned}
&x(0) = x(T) = x(\eta_{max}), && \dot{x}(T) = 0 \\
&u_{min} \leq u(t) \leq u_{max}, && x_{min} \leq x(t) \leq x_{max} \\
&\omega_{ice}(T) = \omega_{ref} \text{ or } \omega_{ice}(t) = \omega_{ref}, && P_{gen}(t) = P_{ref} \\
&P_{ice}(x(t), u(t)) \leq P_{ice,max}(x(t)), && \phi(x(t), u(t)) \leq \frac{1}{\lambda_{min}} \\
&BSR_{min} \leq BSR(x(t), u(t)) \leq BSR_{max}, && \Pi_c \leq \Pi_{c,surge}
\end{aligned} \tag{6}
$$

The constraints are actuator and state limits, as well as constraints imposed by the components, such as maximum power of the engine, P_{ice}, surge-limit of the compressor, $\Pi_{c,surge}$, blade speed ratio-limit of the turbine, BSR, as well as environmental constraints, i.e. an upper limit on ϕ set by the smoke-limiter.

The driving mission-constraints are that the powertrain starts in the operating point of maximum efficiency η_{max}, a point it should also end in, with the added requirement that the end operating point should be stationary. The generator power is also fixed to the reference value. Two types of problems are then studied, one where the engine speed is fixed to the reference speed, denoted $\omega_{ice} = \text{fix}$, and one where it is allowed to depart from this as long as it starts and ends in $\omega_{ice} = \omega_{ref}$, denoted $\omega_{ice} = \text{free}$.

5. NUMERICAL SOLUTION

The software package that is used to solve the optimal control problem numerically is CasADi Andersson [2013]. First the problem is discretized using Radau collocation with three collocation points in each control interval. The states are thus approximated with a third order polynomial, whereas the controls are approximated by a second order polynomial in each control interval. The states are required to be continuous over each control interval boundary, whereas the controls are allowed to be discontinuous. The resulting nonlinear program(NLP) is solved using IPOPT, Wächter and Biegler [2006], with the MA57 linear solver from the HSL package, HSL [2013]. For the wastegate oscillation study 200 control intervals have been used.

6. OSCILLATING CONTROLS

The stationary point of interest here is the one seen with oscillating controls in Fig. 2 namely $P_{gen} = 140$ kW and $\omega_{ice} = 1700$ rpm. The three stationary OCPs (OSS) described in Section 4.1 and the two dynamic OCPs (OSD), $\omega_{ice} = \text{fix}$ and $\omega_{ice} = \text{free}$, described in Section 4.2 are solved using CasADi/IPOPT/HSL and the results are shown in Fig. 3. Looking at Fig. 3 it is clearly visible that both OSDs result in a periodic oscillation. If the engine speed is free the amplitude and frequency changes slightly, however the nature of the oscillation remains the same. The nature of the opening and closing goes against the hypothesis that this should be oscillations due to a singular arc or an effect of the integration error since the wastegate only opens 9-11 times despite 200 control intervals with a three controls in each interval, yielding an optimal period of 90-110ms which is approximately 20 times the control interval length. This indicates that the oscillations are in fact optimal.

This is especially interesting for the case with fixed engine speed, since then the effect can be isolated since all torque

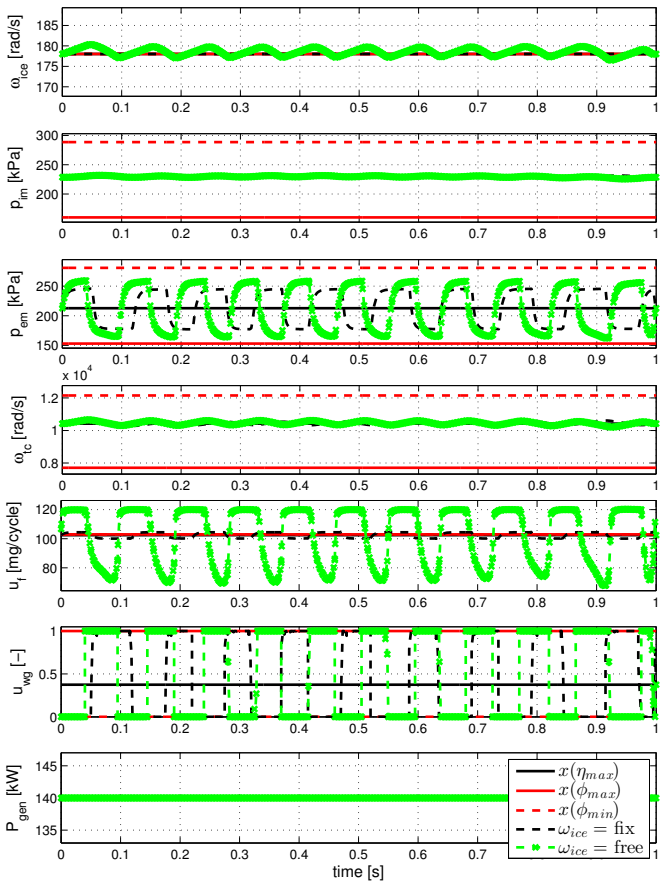

Fig. 3. Optimal states and controls for constant output power, both stationary and dynamic. The dynamic solutions are highly oscillatory.

losses only depend on engine speed except the pumping torque, M_{pump}, see Appendix A.1. This means that the oscillating control actually decreases the pumping torque, as hypothesised in Asprion et al. [2014]. Looking at Fig. 3 the low pass filtering effect of the turbocharger can be clearly seen since the wastegate opening and closing results in a p_{em} span of 60-100 kPa depending on if $\omega_{ice} = \text{free/fix}$, whereas the effect on p_{im} is only 4-5 kPa. In Fig. 4 the pumping power, $P_{pump} = \omega_{ice} M_{pump}$, are shown relative $P_{pump}(\eta_{max})$. Both $x(\phi_{min})$ and $x(\phi_{max})$ increase P_{pump} compared to $x(\eta_{max})$, as expected. The oscillation changes P_{pump} several hundred percent away from what is stationary optimal.

In Table 3 the gains of oscillating controls are quantified. $x(\phi_{max})$ and $x(\phi_{min})$ both increase the pumping energy E_{pump} with 50% which also leads to a relative efficiency decrease of 0.5% (0.2% absolute). The oscillating control with fixed ω_{ice} decreases E_{pump} with 2.4% and ω_{ice} free with 4.1%. Since the friction losses are quadratic in engine speed, ω_{ice}-free, increases the friction losses, but it is still beneficiary since the relative efficiency increase is 0.52‰ vs. 0.24‰ for ω_{ice}-fix (0.2‰ vs. 0.09‰ absolute).

The gains are small but nevertheless surprising since it's a dynamic phenomenon. Looking at Fig. 5 the wastegate's effect on the stationary efficiency as well as pumping torque is shown. The efficiency is a convex function in u_{wg} whereas M_{pump} is concave, which if the analysis was per-

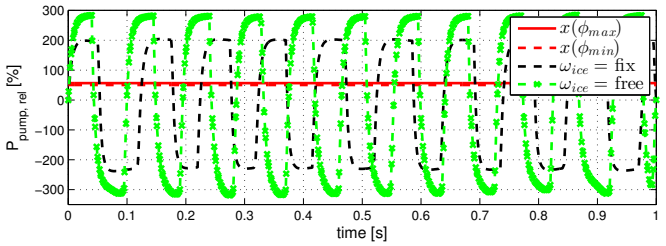

Fig. 4. Pumping power relative the stationary optimal point.

	$\Delta\eta$	ΔE_{fric}	ΔE_{pump}	ΔE_{ig}
$x(\phi_{max})$	-0.542	0.0	56.3782	0.5448
$x(\phi_{min})$	-0.482	0.0	50.1279	0.4844
ω_{ice} = fix	0.024	0.0	-2.4073	-0.0223
ω_{ice} = free	0.052	0.8797	-4.0869	-0.0263

Table 3. Changes in efficiency and energies relative $x(\eta_{max})$ in percent, $E_x = \int_0^T P_x \, dt$.

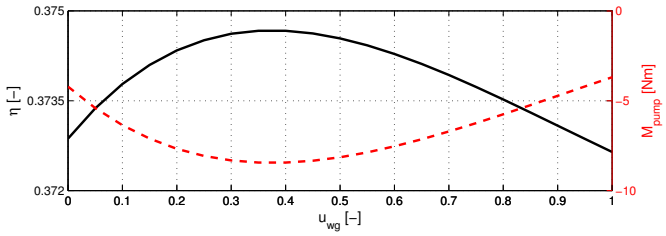

Fig. 5. Wastegate position's effect on the efficiency and pumping torque during stationary conditions.

formed for stationary conditions would lead to the conclusion that oscillating controls would increase the pumping torque and consequently decrease the efficiency. However the result is actually the opposite, oscillating between the two worst controls from a stationary perspective, increases the efficiency dynamically.

7. MODEL EXTENSIONS

To investigate whether the oscillating controls are results of a modeling assumption a set of different model extensions are considered. The extensions and their motivation are:

- x_r: Model for residual gas: In Sivertsson and Eriksson [2014] it is shown that mean/max absolute relative error increase of assuming $x_r = 0$ is [0.014/0.06] ‰ versus measurements. However in the oscillating controls the exhaust pressure changes very rapidly, something that might have a significant effect on the amount of residual gas trapped in the cylinder.
- $\eta_{vol,2}$: Pressure ratio dependent volumetric efficiency model. In the volumetric efficiency model used, see Appendix A.2, only the dependence of the intake manifold pressure and engine speed are modeled. Of course the changing pressure ratio over the engine could have effects on the volumetric efficiency.
- Adiabatic: The isothermal exhaust manifold model used, see Appendix A.3, neglects energy conservation since it assumes that the gases flowing in and out of the control volume have the same temperature, therefore an adiabatic exhaust manifold model that satisfies both conservation of mass and energy is implemented.

The basic model is $MVEM_o$ which is then extended with different combinations of these three models. The model fit for the different models versus both dynamic(Dyn.) and stationary measurements(Stat) are shown in Table 4. None of the model extensions have any significant effects on the model fit versus measurements.

7.1 Residual gas

In Wahlström and Eriksson [2011] the engine out temperature model is based on an ideal Seiliger cycle model, incorporating residual gas. The model is formulated as:
$x_{r,0} = 0, T_{eo,0} = 800$.
While $\|T_{eo,k+1} - T_{eo,k}\| >$1e-6

$$\begin{aligned}
q_{in} =& \frac{\dot{m}_f q_{HV}}{\dot{m}_f + \dot{m}_{ac}}(1 - x_{r,k}) \\
x_p =& 1 + \frac{q_{in} x_{cv}}{c_{v,a} T_1 r_c^{\gamma_a - 1}} \\
x_v =& 1 + \frac{q_{in}(1 - x_{cv})}{c_{p,a}(\frac{q_{in} x_{cv}}{c_{v,a}} + T_1 r_c^{\gamma_a - 1})} \\
x_{r,k+1} =& \frac{\Pi_e^{1/\gamma_a} x_p^{-1/\gamma_a}}{r_c x_v} \\
T_1 =& x_{r,k+1} T_{eo,k} + (1 - x_{r,k+1}) T_{im} \\
T_{eo,k+1} =& \eta_{sc} \Pi_e^{1-1/\gamma_a} r_c^{1-\gamma_a} x_p^{1/\gamma_a - 1} \\
& \left(q_{in} \left(\frac{1 - x_{cv}}{c_{p,a}} + \frac{x_{cv}}{c_{v,a}} \right) + T_1 r_c^{\gamma_a - 1} \right)
\end{aligned} \tag{7}$$

The equations in (7) are nonlinear and depend on each other and need to be solved using fixed point iterations. In Wahlström and Eriksson [2011] it is shown that if the solution from the previous time step is known, one iteration suffices to get a good approximation of the engine out temperature. In an optimization context it is difficult to keep track of the solution form the previous time step since the time steps are solved simultaneously. Also a submodel that is evaluated for a varying number of iterations is undesirable, especially since it complicates the computation of derivatives. Therefore this type of model is not implementable in an optimization context and a new model is developed.

x_r is modeled as a function of both pressure ratio over the engine and the fuel to mass ratio. defined as:

$$MFR = \frac{\dot{m}_f}{\dot{m}_f + \dot{m}_{ac}} \tag{8}$$

$$x_r = \frac{x_{r,mod1}}{x_{r,mod2}} = \frac{c_{x_{r1}} \Pi_e^2 + c_{x_{r2}} \Pi_e + c_{x_{r3}}}{1 + c_{x_{r4}} MFR} \tag{9}$$

In Fig. 6-top this gives a good agreement to the iterative model, resulting in mean/max relative errors of [0.92/4.52] %. Using that x_{cv} becomes zero in the optimization for this particular engine T_{eo} can be computed according to

$$T_{eo} = \frac{(1 - x_r)(\frac{q_{HV} MFR}{c_{p,a}} + T_{im} r_c^{\gamma_a - 1})}{\frac{1}{\eta_{sc} \Pi_e^{1-1/\gamma_a} r_c^{1-\gamma_a}} - x_r r_c^{\gamma_a - 1}} \tag{10}$$

T_{eo} and x_r could be used as starting values and then one iteration of the fixed point iteration can be performed. However it turns out that not only is it more computations,

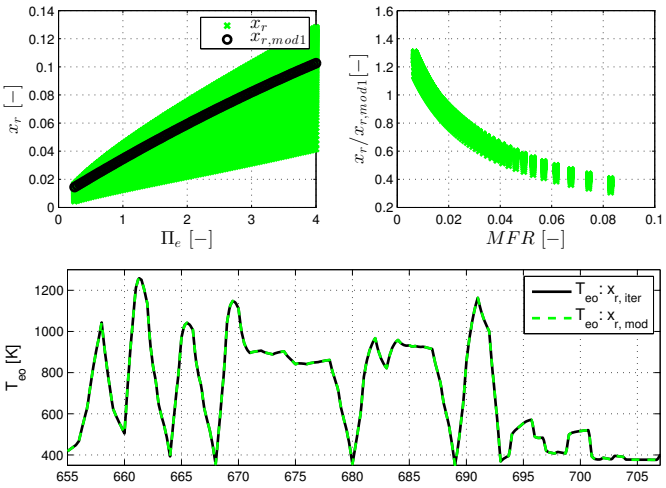

Fig. 6. Top: Residual gas, x_r, vs. pressure ratio, Π_e, and how this dependence is modeled (Left). The x_r error's dependence on MFR (Right). Bottom: Fit of the new residual gas model for phase 8 of the WHTC.

the model fit is actually worse. When simulated over the entire WHTC the mean/max absolute relative error of exhaust gas temperature, T_{eo} for the model in (8)-(10) relative the model in (7) are [0.025/0.22]%. If in addition to (8)-(10) one fixed point iteration is used the errors increase to [0.045/0.34] %. The model used is therefore the one without iterations. In Fig. 6-bottom the fit vs. the model in (7) is shown.

7.2 $\eta_{vol,2}$: Modified volumetric efficiency

The $\eta_{vol,2}$ model implemented is a modified version of the model found in Eriksson and Nielsen [2014], consisting of an ideal part and two polynomials, in ω_{ice} and p_{im} respectively.

$$\eta_{vol,ideal} = \frac{r_c - \left(\frac{p_{em}}{p_{im}}\right)^{1/\gamma_a}}{r_c - 1}$$
$$\eta_{vol,\omega_{ice}} = c_{\eta_{vol,1}}\omega_{ice}^2 + c_{\eta_{vol,2}}\omega_{ice} + c_{\eta_{vol,3}}$$
$$\eta_{vol} = \eta_{vol,\omega_{ice}}\eta_{vol,ideal} + c_{\eta_{vol,4}}p_{im} + c_{\eta_{vol,5}}$$

The component model fit for stationary measurements are slightly better than the model in (A.10), with mean/max absolute relative errors of 0.62/2.68 % vs. 0.9/3.7 % for (A.10), which is to be expected since the number of tuning parameters increases from three to five.

7.3 Adiabatic exhaust manifold model

The adiabatic model, as described in Chevalier et al. [2000] is implemented according to:

$$\frac{dp_{em}}{dt} = \frac{R_e\gamma_e}{V_{em}}\left(T_{em,k}\left(\dot{m}_{ac}+\dot{m}_f\right) - T_{em}\left(\dot{m}_t+\dot{m}_{wg}\right)\right)$$
$$\frac{dT_{em}}{dt} = \frac{R_eT_{em}}{p_{em}V_{em}}\Bigg(\gamma_e\Big(T_{em,k}\left(\dot{m}_{ac}+\dot{m}_f\right) - T_{em}\left(\dot{m}_t+\dot{m}_{wg}\right)\Big)$$
$$- T_{em}(\dot{m}_{ac}+\dot{m}_f-\dot{m}_t-\dot{m}_{wg})\Bigg)$$

This means extending the model with an additonal state, T_{em}. $T_{em,k}$, i.e. the temperature of the gases flowing into the manifold is computed according to (A.13), that is temperature after heat loss.

Table 4. Mean absolute relative errors for the different models versus measurements. T=tuning set, V=validation set.

	ω_{ice}		p_{im}		p_{em}		ω_{tc}	
Dyn.	T	V	T	V	T	V	T	V
$MVEM_o$	0.0	0.0	2.8	2.2	2.8	2.9	2.9	2.9
x_r	0.0	0.0	2.8	2.2	2.8	2.9	2.9	2.9
x_r+adiabatic	0.0	0.0	2.8	2.2	2.8	3.0	2.9	3.0
$\eta_{vol,2}$	0.0	0.0	2.8	2.3	2.9	3.0	3.0	3.2
$\eta_{vol,2}+x_r$+adiabatic	0.0	0.0	2.9	2.3	2.9	3.0	3.1	3.2
Stat.	$\dot{m}_c$	P_c	$\dot{m}_{ac}$	T_{em}	$\dot{m}_{exh}$	P_t	P^+_{mech}	P^-_{mech}
$MVEM_o$	2.5	1.8	2.5	2.4	3.3	5.4	3.4	1.4
x_r	2.5	1.8	2.4	2.5	3.3	5.5	3.3	1.5
x_r+adiabatic	2.5	1.8	2.5	2.7	3.1	4.9	3.1	1.5
$\eta_{vol,2}$	2.5	2.0	2.7	2.3	3.2	5.5	5.1	1.4
$\eta_{vol,2}+x_r$+adiabatic	2.5	1.9	2.7	2.6	3.0	4.9	4.4	1.6

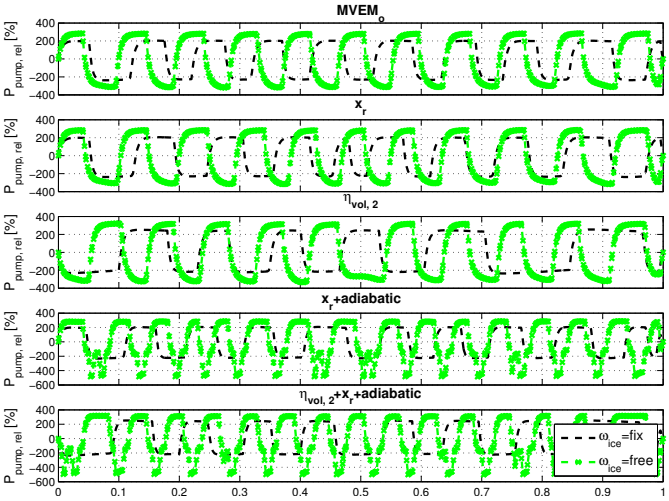

Fig. 7. Relative pumping power of the optimal solutions to the two OSDs for the different models, relative the stationary optimal operating point. The oscillatory solution can not be explained by any of the model extensions.

8. RESULTS

The two OSDs defined in Section 4.2 are solved for the different models and the resulting optimal pumping power, P_{pump} is plotted relative the stationary optimal in Fig. 7. The oscillations cannot be explained by any of the model extensions. The periodic nature of the solution is present for all model extensions and the changes in frequency and amplitude of the oscillations are minor. In Table 5 the changes in energies and efficiency are shown, which confirms the results seen in Fig. 7. The decrease in pumping energy, ΔE_{pump}, increases for each model extension for ω_{ice} = fix, indicating that given a standard mean value engine model it actually is optimal to use periodic wastegate control in order to decrease the pumping torque.

9. CONCLUSIONS

Optimal control of a diesel-electric powertrain is studied. It is shown that the oscillatory solutions seen for certain operating points are not directly discretization dependent. Instead the solution is periodic with a period much greater than the control interval length. Further it is seen that

Table 5. Changes in efficiency and energies of the two OSDs, ω_{ice} = fix and ω_{ice} = free, relative $x(\eta_{max})$, for the different models.

		$\Delta\eta$	ΔE_{fric}	ΔE_{pump}	ΔE_{ig}
$MVEM_o$	fix	0.024	0.0	-2.41	-0.02
	free	0.052	0.88	-4.09	-0.03
x_r	fix	0.024	0.0	-2.52	-0.02
	free	0.054	1.32	-3.64	0.02
x_r+ adiabatic	fix	0.024	0.0	-2.58	-0.02
	free	0.068	1.74	-3.7	0.19
$\eta_{vol,2}$	fix	0.029	0.0	-3.14	-0.03
	free	0.070	-2.23	-10.16	-0.31
$\eta_{vol,2} + x_r$+ adiabatic	fix	0.030	0.0	-3.23	-0.03
	free	0.080	-1.99	-10.21	-0.22

the pumping work of the engine decreases as a result of the oscillations. To study if this effect is a result of over-simplification in the previously published mean value engine model, several model extensions are investigated and their corresponding optimal control problems are solved. Furthermore a new residual gas model, suitable for optimal control, is presented. It is shown that the oscillating controls cannot be explained by the implemented extensions to the previously published model, showing that for certain operating points for mean value engine models the optimal solution is actually periodic.

REFERENCES

Joel Andersson. *A General-Purpose Software Framework for Dynamic Optimization*. PhD thesis, Arenberg Doctoral School, KU Leuven, Department of Electrical Engineering (ESAT/SCD) and Optimization in Engineering Center, Kasteelpark Arenberg 10, 3001-Heverlee, Belgium, October 2013.

Jonas Asprion, Oscar Chinellato, and Lino Guzzella. Optimal control of diesel engines: Numerical methods, applications, and experimental validation. *Mathematical Problems in Engineering*, 2014.

Alain Chevalier, Martin Müller, and Elbert Hendricks. On the validity of mean value engine models during transient operation. In *SAE Technical Paper 2000-01-1261*. SAE International, 2000.

Lars Eriksson and Lars Nielsen. *Modeling and Control of Engines and Drivelines*. John Wiley & Sons, 2014.

Elmer G. Gilbert. Vehicle cruise: Improved fuel economy by periodic control. *Automatica*, 12:159–166, 1976.

Elmer G. Gilbert. Optimal periodic control: A general theory of necessary conditions. *SIAM Journal of Control and Optimization*, 15(5):717–746, 1977.

Erik Hellström, Jan Åslund, and Lars Nielsen. Design of an efficient algorithm for fuel-optimal look-ahead control. *Control Engineering Practice*, 18(11):1318–1327, 2010.

HSL. A collection of fortran codes for large scale scientific computation. http://www.hsl.rl.ac.uk, 2013.

Adam Lowell Schwartz. *Theory and implementation of numerical methods based on Runge-Kutta integration for solving optimal control problems*. PhD thesis, University of Berkeley, California, 1996.

Martin Sivertsson and Lars Eriksson. Modeling for optimal control: A validated diesel-electric powertrain model. In *SIMS 2014 - 55th International Conference on Simulation and Modelling*, Aalborg, Denmark, 2014.

Martin Sivertsson and Lars Eriksson. Optimal transient control trajectories in diesel-electric systems-part 1: Modeling, problem formulation and engine properties. *Journal of Engineering for Gas Turbines and Power*, 137(2), February 2015a.

Martin Sivertsson and Lars Eriksson. Optimal transient control trajectories in diesel-electric systems-part 2: Generator and energy storage effects. *Journal of Engineering for Gas Turbines and Power*, 137(2), February 2015b.

Vehicular systems software. "`http://www.fs.isy.liu.se/Software/`", 2014.

Andreas Wächter and Lorenz T. Biegler. On the implementation of an interior-point filter line-search algorithm for large-scale nonlinear programming. *Mathematical Programming*, 106:25–57, 2006.

Johan Wahlström and Lars Eriksson. Modelling diesel engines with a variable-geometry turbocharger and exhaust gas recirculation by optimization of model parameters for capturing non-linear system dynamics. *Proceedings of the Institution of Mechanical Engineers, Part D, Journal of Automobile Engineering*, 225(7):960–986, 2011.

WHDC Working Group. Worldwide harmonized heavy duty emissions certification procedure. "`http://www.unece.org/fileadmin/DAM/trans/doc/2005/wp29grpe/TRANS-WP29-GRPE-50-inf04r1e.pdf`", 2005. GRPE-50-4-Rev.1, Read 2/2-2015.

Appendix A. EXCERPTS FROM ORIGINAL MODEL

A.1 Torque model

$$M_{ice} = M_{ig} - M_{fric} - M_{pump} \tag{A.1}$$

$$M_{pump} = \frac{V_d}{4\pi}\left(p_{em} - p_{im}\right) \tag{A.2}$$

$$M_{fric} = \frac{V_d}{4\pi}10^5\left(c_{fr1}\omega_{ice}^2 + c_{fr2}\omega_{ice} + c_{fr3}\right) \tag{A.3}$$

$$M_{ig} = \frac{u_f 10^{-6} n_{cyl} q_{HV} \eta_{ig}}{4\pi} \tag{A.4}$$

$$\eta_{ig} = \eta_{ig,t}(1 - \frac{1}{r_c^{\gamma_{cyl}-1}}) \tag{A.5}$$

$$\eta_{ig,t} = M_{f,1} + g_f\left(M_{f,2} - M_{f,1}\right) \tag{A.6}$$

$$g_f = \frac{1 + \tanh(0.1(\omega_{ice} - 1500\pi/30))}{2} \tag{A.7}$$

$$M_{f,1} = c_{M_{f,1},1}\omega_{ice}^2 + c_{M_{f,1},2}\omega_{ice} \tag{A.8}$$

$$M_{f,2} = c_{M_{f,2},1}\omega_{ice}^2 + c_{M_{f,2},2}\omega_{ice} + c_{M_{f,2},3} \tag{A.9}$$

A.2 Volumetric efficiency

$$\eta_{vol} = c_{vol,1}\sqrt{p_{im}} + c_{vol,2}\sqrt{\omega_{ice}} + c_{vol,3} \tag{A.10}$$

A.3 Exhaust pressure and temperature

$$q_{in} = \frac{\dot{m}_f q_{HV}}{\dot{m}_f + \dot{m}_{ac}} \tag{A.11}$$

$$T_{eo} = \eta_{sc}\Pi_e^{1-1/\gamma_a} r_c^{1-\gamma_a}\left(\frac{q_{in}}{c_{p,a}} + T_{im} r_c^{\gamma_a - 1}\right) \tag{A.12}$$

$$T_{em} = T_{amb} + (T_{eo} - T_{amb})e^{-\frac{h_{tot}V_{pipe}}{(\dot{m}_f + \dot{m}_{ac})c_{p,e}}} \tag{A.13}$$

$$\frac{dp_{em}}{dt} = \frac{R_e T_{em}}{V_{em}}\left(\dot{m}_{ac} + \dot{m}_f - \dot{m}_t - \dot{m}_{wg}\right) \tag{A.14}$$